Performance of ATLAS RPC detectors and L1 Muon Barrel Trigger with a new CO2-based gas mixture

Eric Ballabene
on behalf of the ATLAS Collaboration
University and INFN, Bologna

Outline

- The ATLAS Muon RPC detector and the RPC trigger
- The RPC detector during Run3 (2022-2025)
  - The gas mixture change
  - The HV correction factor
- Detector performance:
  - density of current of the gas gaps
  - cluster size at module level
- Trigger performance:
  - Trigger efficiency across runs
  - Trigger efficiency p_{T} turn-on curves
  - η vs φ trigger efficiency maps
- Conclusions

The ATLAS RPC Detector

The RPC detector is a large planar capacitor with two parallel high resistivity **electrode plates** (~10^{10} Ω cm) separated by a set of insulating spacers, defining a gas gap of 2 mm.

The gap is filled with a **suitable gas mixture** at atmospheric pressure representing the target for the ionizing radiation.

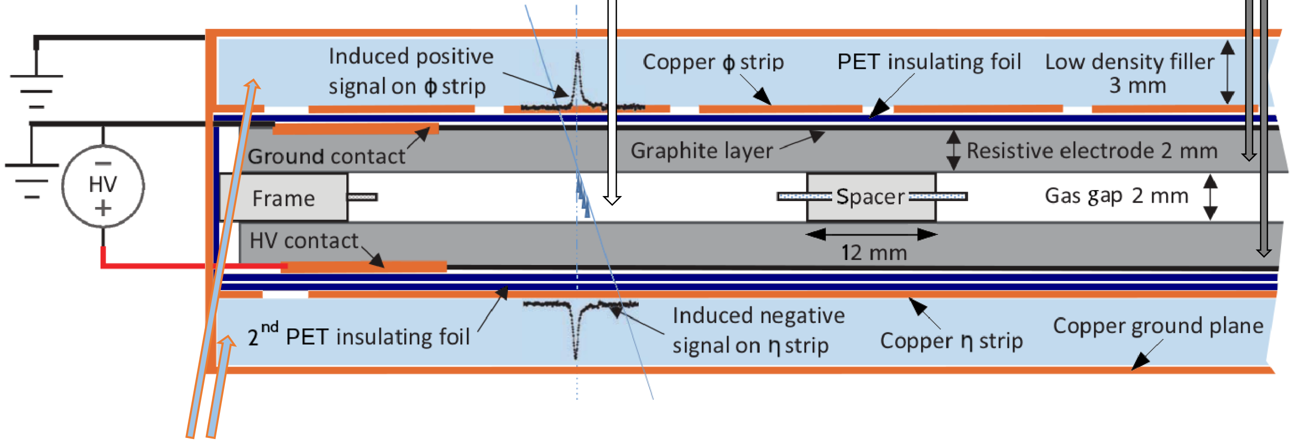

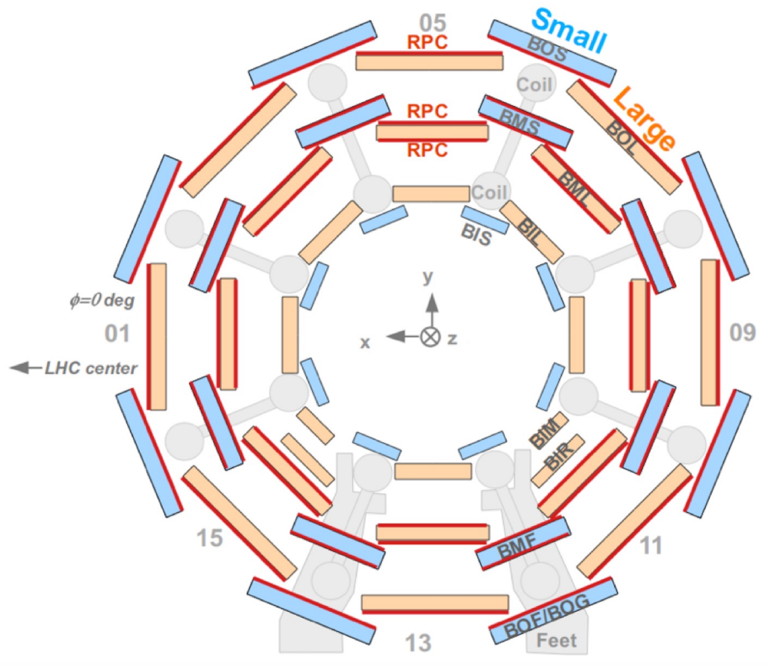

Readout panels are made with η- or φ-oriented strips on both sides of the gas gap with FE electronics.

The RPC system consists of **doublet chambers**, each composed of two RPC gas gap readouts.

Two RPC doublets are attached to the two sides of the middle layer of MDT chambers (BM), and the third one to one side of the outer MDT layer (BO).

The RPC Trigger

The RPC system provides the L1 hardware muon trigger in the barrel. Two types of muon triggers:

- **Low-p_T** triggers require a coincidence between two of the innermost chambers in BM.
- **High-p_T** triggers require a coincidence between a BM pivot chamber and a BO chamber.

The barrel trigger system is sub-divided into 432 projective towers, each provided with on-detector trigger and readout electronics boards containing the processor boxes (PADs) for low- and high-p_T triggers.

The hit coincidences are implemented by custom coincidence-matrix ASICs (CMAs) in the PAD boxes. The CMAs align the FE signals in time, check the time coincidence of RPC hits and perform trigger logic operations.

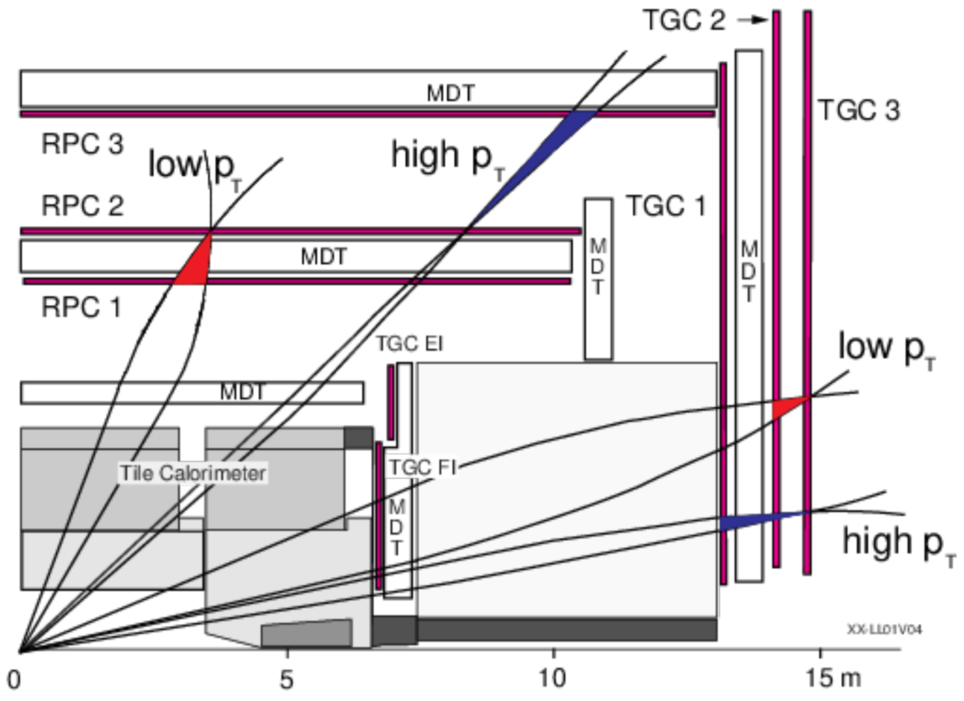

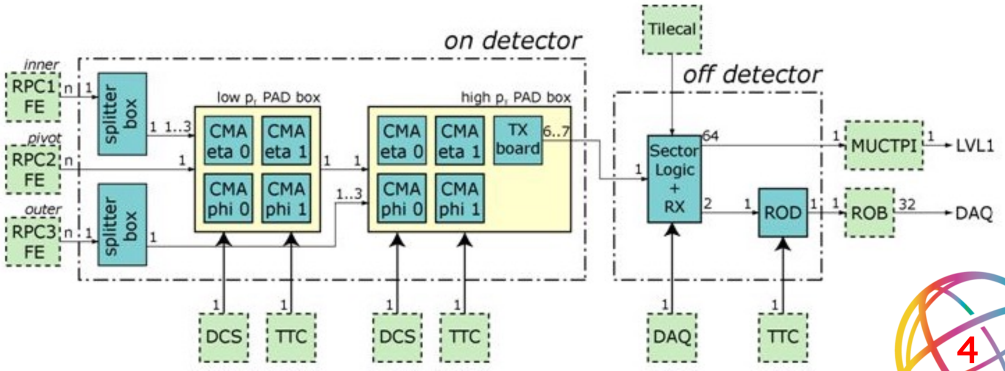

The RPC detector in Run3

After a successful data taking period in Run2, the detector has undergone an intense maintenance to ensure an efficient data taking during Run3.

Several interventions have been carried out on the detector, mainly covering the gas distribution with the aim of stabilizing the system and reducing the amount of gas released in the atmosphere [see also "*Mitigation of the ATLAS RPC environmental impact*" talk].

The main interventions were:

- Change of gas mixture adding a CO_2 gas fraction;
- New gas distribution racks have been added to increase the vertical segmentation and in view of the installation of new Phase-II chambers;
- Non-return valves have been installed on the chamber outputs to avoid reverse flow with large leaks;
- A massive gas leak repair campaign has been done for fixing the continuously developing leaks;
- A new technique to repair and prevent new leaks has been tested;
- The segmentation of the HV channels has been doubled in a third of the spectrometer to mitigate the effect of detector failures.

The RPC gas mixture

The RPCs are continuously flushed with a gas mixture of:

- $C_2H_4F_4$, the gas target for the primary ionization;
- i-C_4H_{10}, a quencher component that helps to avoid propagation of the discharge;
- SF_6, an electronegative component that helps to limit the growth of avalanches.

This gas mixture has a strong greenhouse effect, and it is currently being phased down in the European Union, thereby also leading to rising cost.

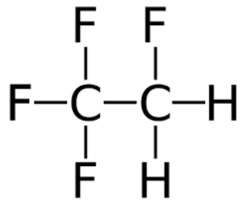

$C_2H_4F_4$ (R-134a)
GWP: 1430

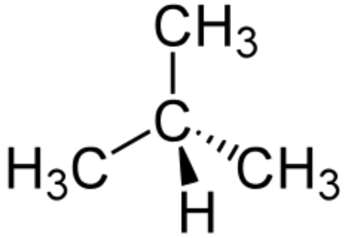

i-C_4H_{10}
GWP: 3.3

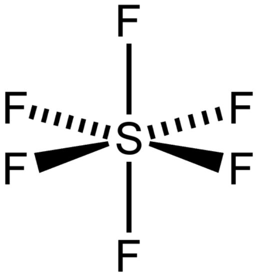

SF_6
GWP: 22800

The gas mixture was changed in August 2023 during Run3:

from $C_2H_4F_4$ 94.7%, i-C_4H_{10} 5%, SF_6 0.3%

to $C_2H_4F_4$ 64%, CO_2 30%, i-C_4H_{10} 5%, SF_6 1%.

The new gas mixture foresees a **~14%** reduction of the Global Warming Potential (GWP). The average applied voltage across all detector chambers was 9.6 kV before the gas mixture change, while the new applied voltage is **9.35 kV**. The effective operational voltage is corrected for local changes in environmental temperature and pressure with respect to the standard conditions.

The HV correction factor

- The effective operational voltage V_{eff} is corrected for local changes in environmental pressure p and temperature T at the chamber level by the HV correction factor $\rho(p,T)$.
- The applied operational voltage V_{app} is therefore given by:

$$V_{\text{app}} = V_{\text{eff}}\,\rho(p,T),$$

where

$$\rho(p,T) = \left[1 + \alpha_p\left(\frac{p}{p_0} - 1\right)\right]\left[1 + \alpha_T\left(\frac{T_0 - 273.15}{T - 273.15} - 1\right)\right].$$

In the formula, $\alpha_p = 0.8$, $\alpha_T = 0.5$, $p_0 = 9.6 \cdot 10^4$ Pa, $T_0 = 294.15$ K, $V_{\text{eff}} = 9350\ \text{V}$ and $0.98 \leq \rho(p,T) \leq 1.02$.

- During May 2024, the HV correction factor $\rho(p,T)$ was updated to take into account a new pressure probe and local changes of pressure and temperature for the BO chambers whose segmentation for the HV channels has been doubled.
- The updated HV correction factor led to an increase between ~30V and ~150V for some of the RPC chambers, resulting in an increase of the mean gas gap current density and improving the stability of the RPC trigger efficiency.

Density of gas gap current

- The addition of the CO_2 leads to an increase of the current density of the gas gaps of around **~17%** in agreement with prototype results, even if the operational voltage has been lowered with the new gas mixture, without decreasing the muon detection efficiency.

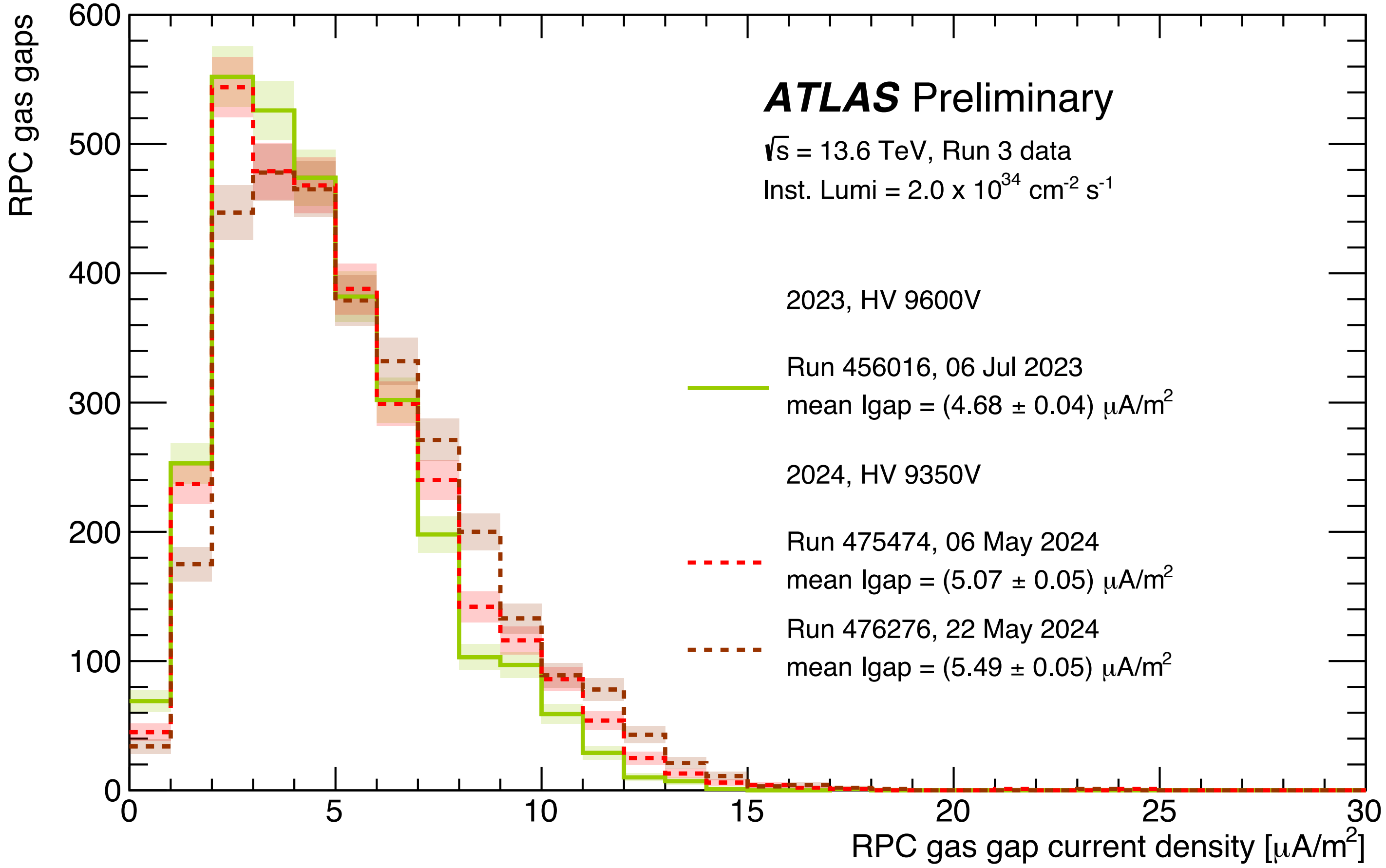

Distributions of the measured current density for all the RPC gas gaps at the instantaneous luminosity of 2.0×10^{34} cm^{-2}s^{-1} for 3 different Runs:

- Run 45016 (2023);
- Run 475474 (2024, before the updated HV correction factor);
- Run 476276 (2024, after the updated HV correction factor).

Density of gas gap current

- Linear increase of the RPC mean gap current density as a function of the instantaneous luminosity.

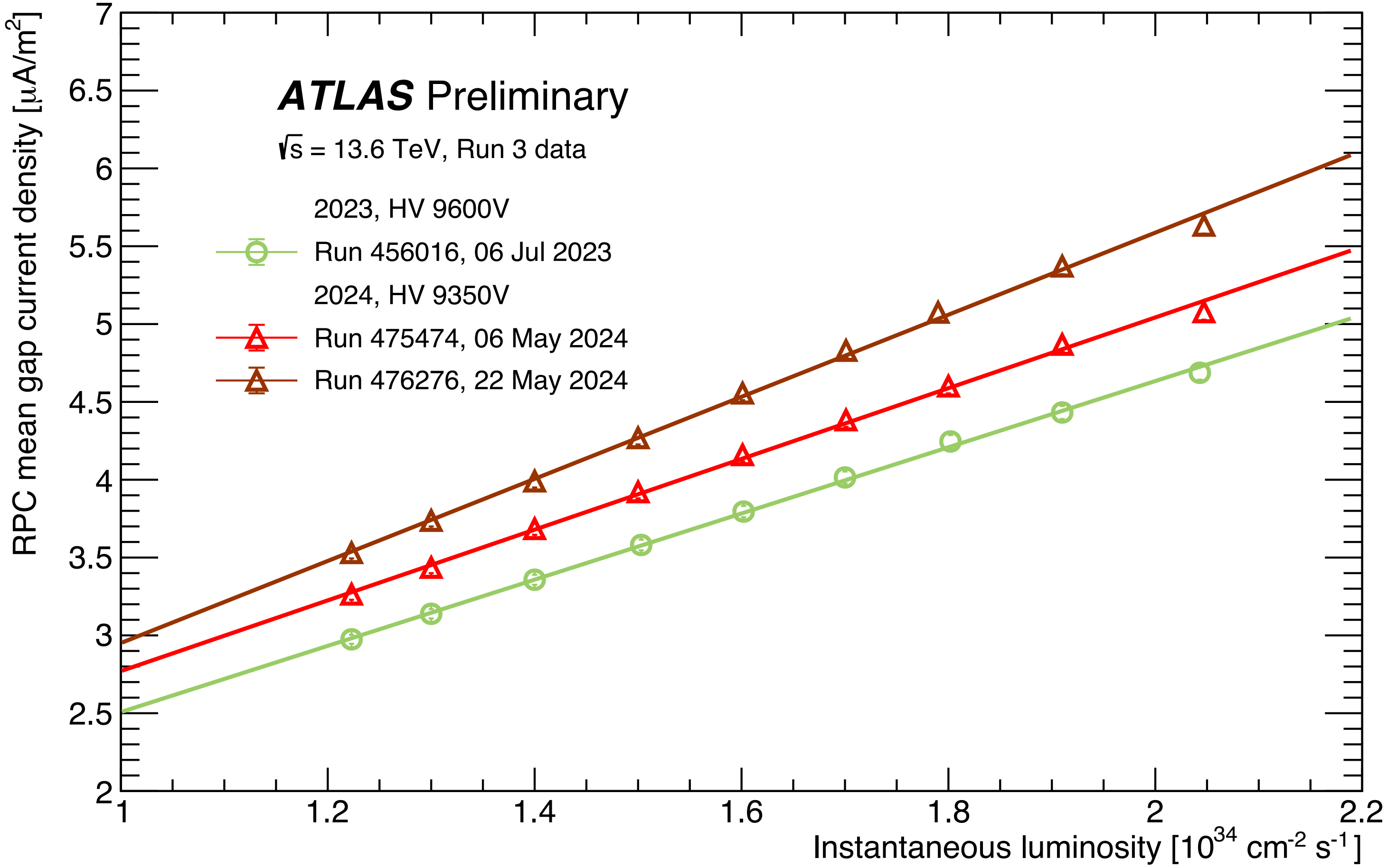

Measured current density for all the RPC gas gaps as a function of the instantaneous luminosity for 3 different Runs:

- Run 45016 (2023);
- Run 475474 (2024 before the updated HV correction factor);
- Run 476276 (2024 after the updated HV correction factor).

Cluster size at module level

- The addition of CO_2 would increase the cluster size but the increased SF_6 component in the gas mixture limits the dimension of the avalanche. The combined effect yields a similar cluster size between 2023 and 2024, smaller in 2024 than in 2023. No signs of detector ageing effects yet.

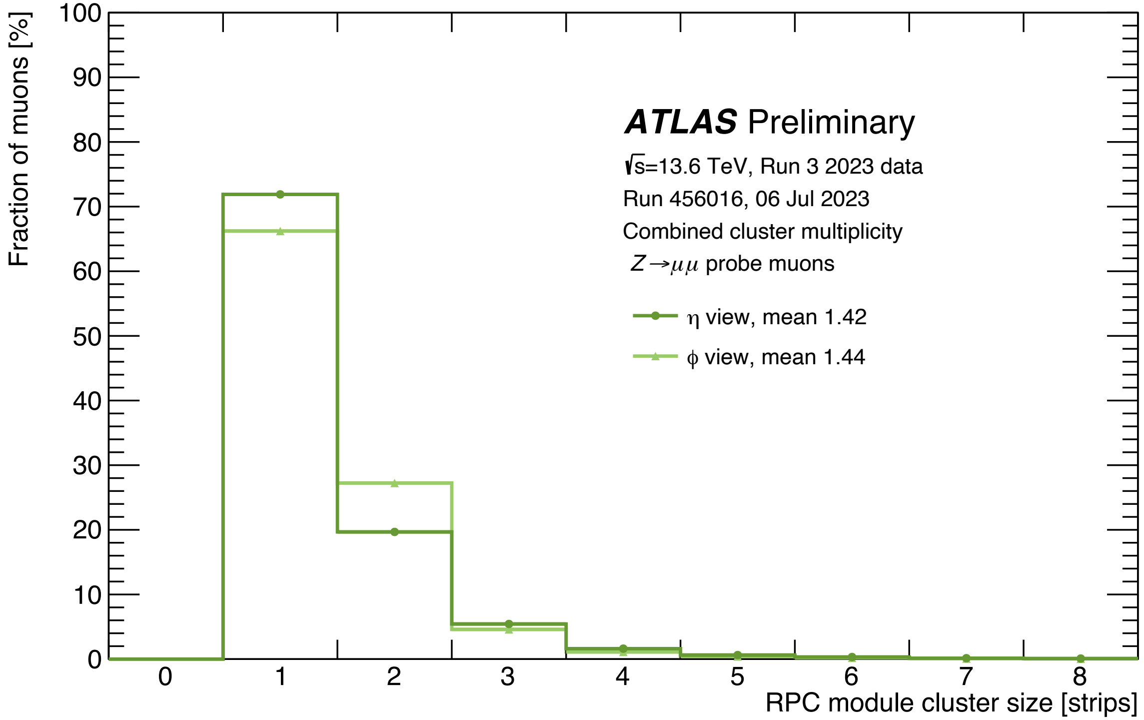

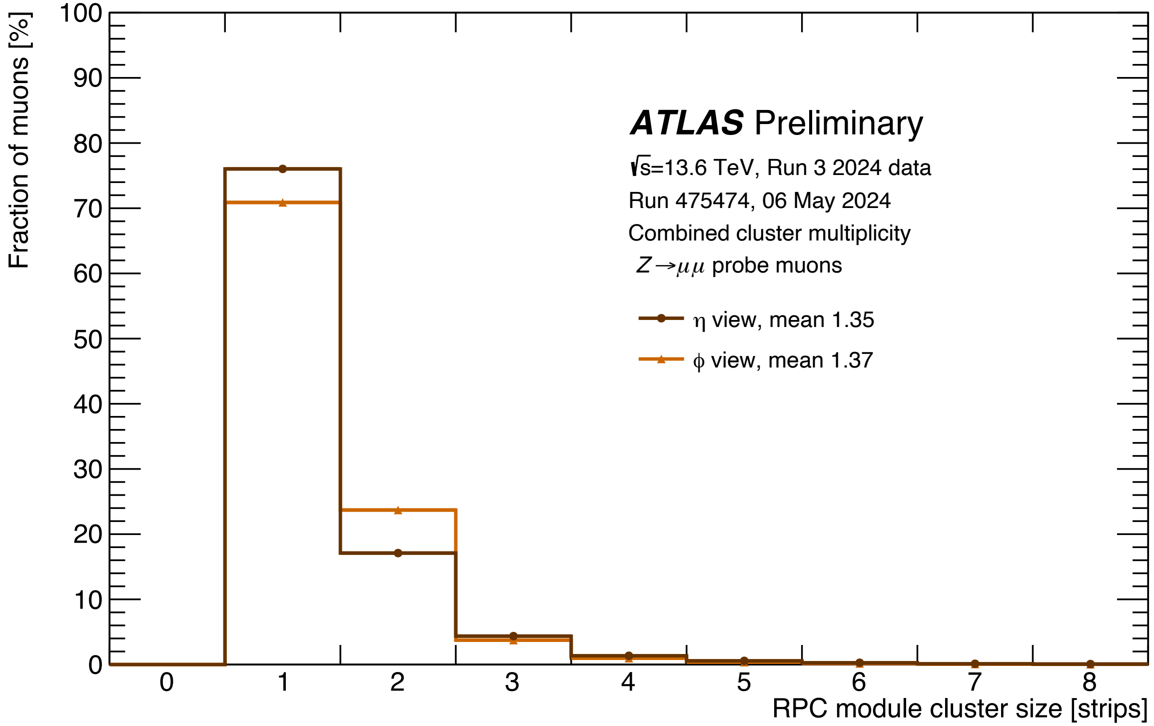

Cluster size distributions for Run 456016 (2023, left) and for Run 475474 (2024, right).

Trigger performance

- RPC trigger efficiency fairly constant during 2023 and 2024, fluctuating from run to run.
- Instabilities in 2024 were fixed by an improved version for the handling of the HV correction factor ρ.

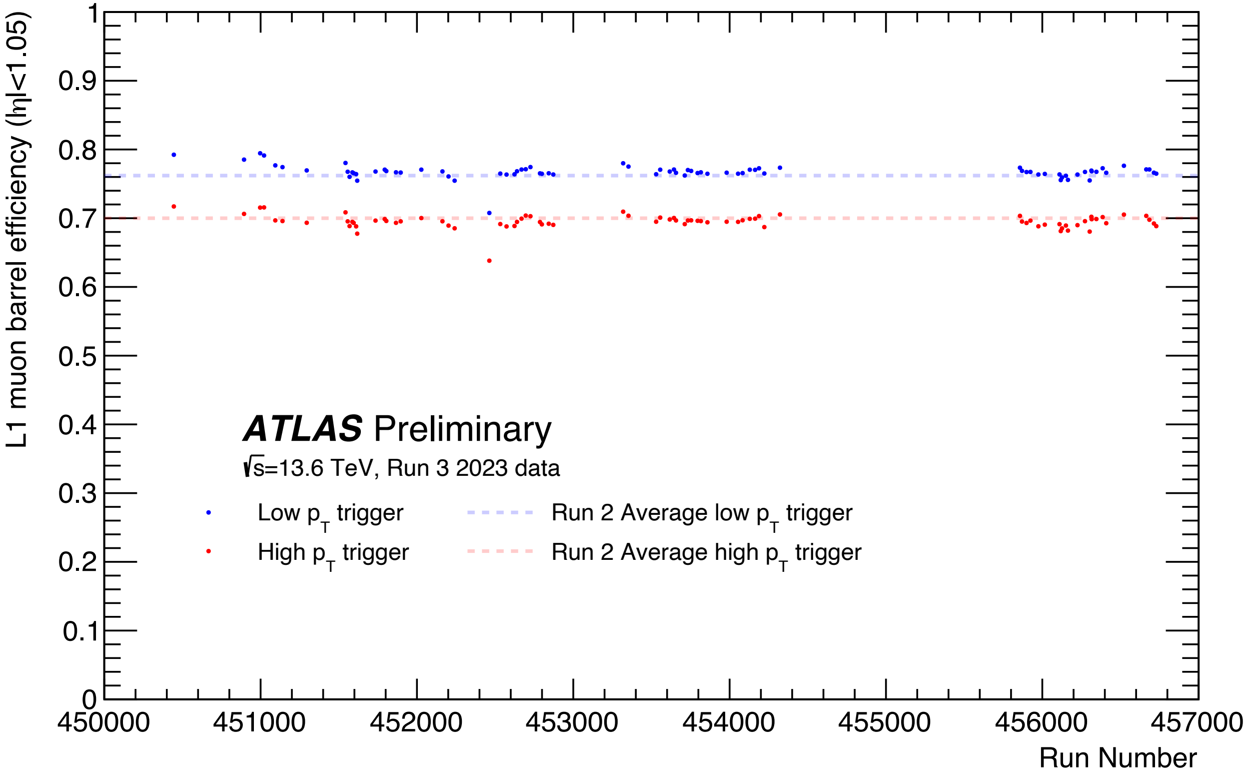

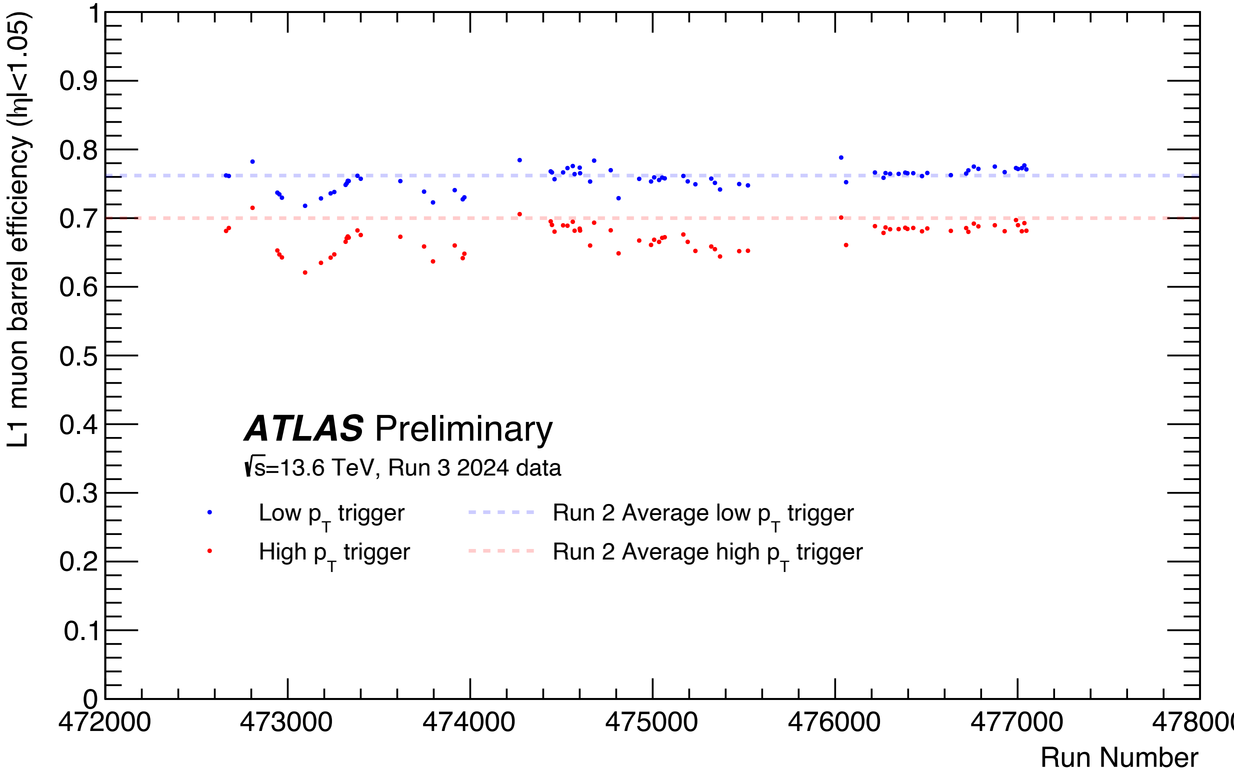

L1 muon barrel trigger efficiency (efficiency including acceptance) for 2023 (left) and 2024 (right) as a function of the Run Number, obtained with non-muon triggers on the physics main-stream.

Trigger performance - p_T turn-on curves

- Constant trigger performance between 2023 and 2024 for the different Run3 L1 trigger thresholds.

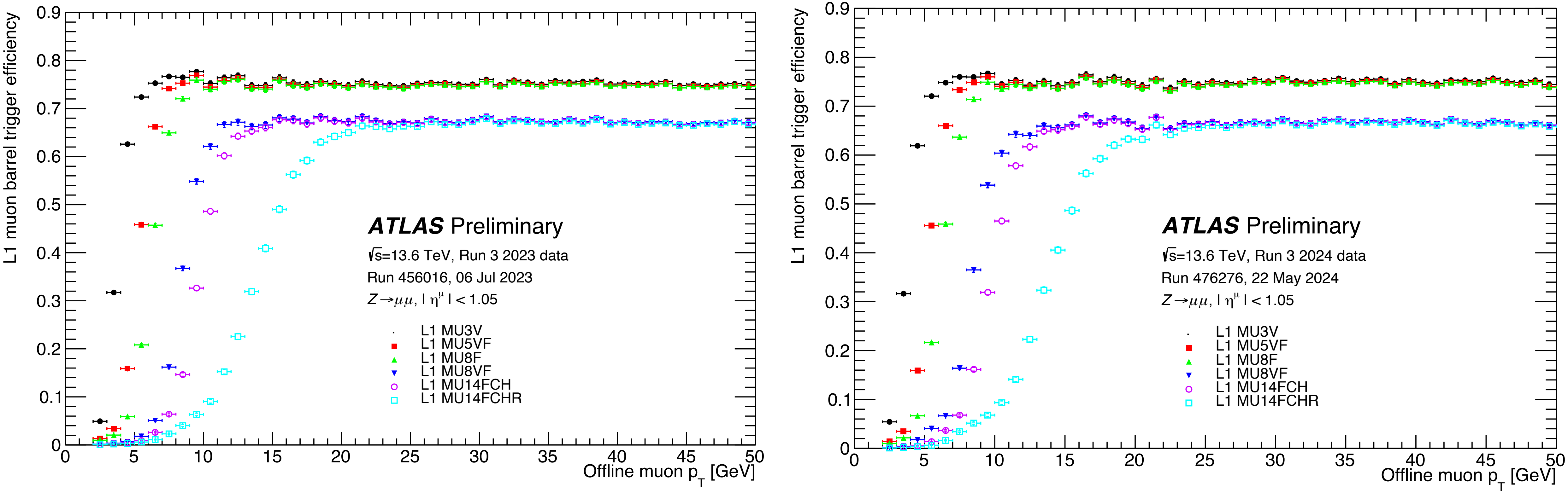

L1 muon barrel trigger efficiency as a function of the offline muon p_T for Run 456016 (2023, left) and for Run 476276 (2024, right) for different L1 triggers used in Run 3.

Trigger performance - high p_T $\eta - \varphi$ efficiency maps

- Constant trigger performance between 2023 and 2024 for high p_T triggers.
- Improvement in trigger coverage due to the YETS interventions.

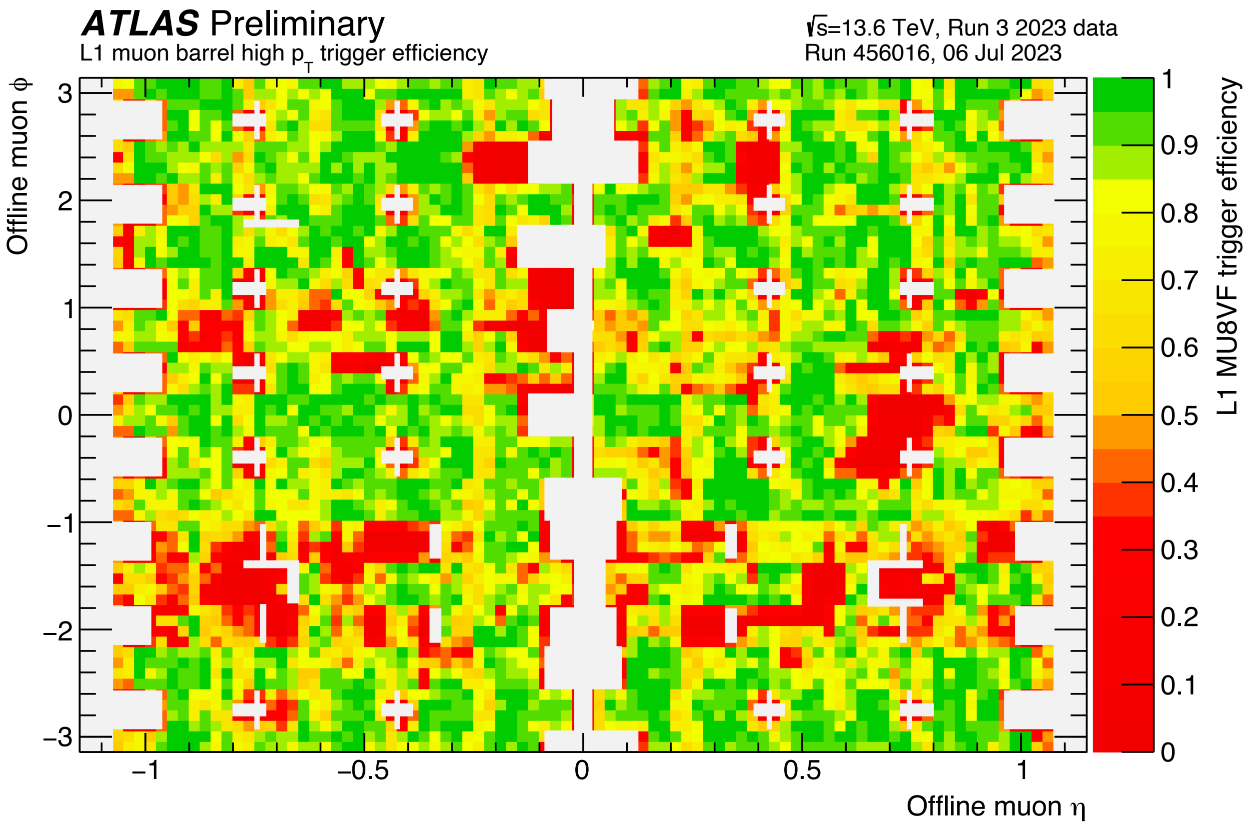

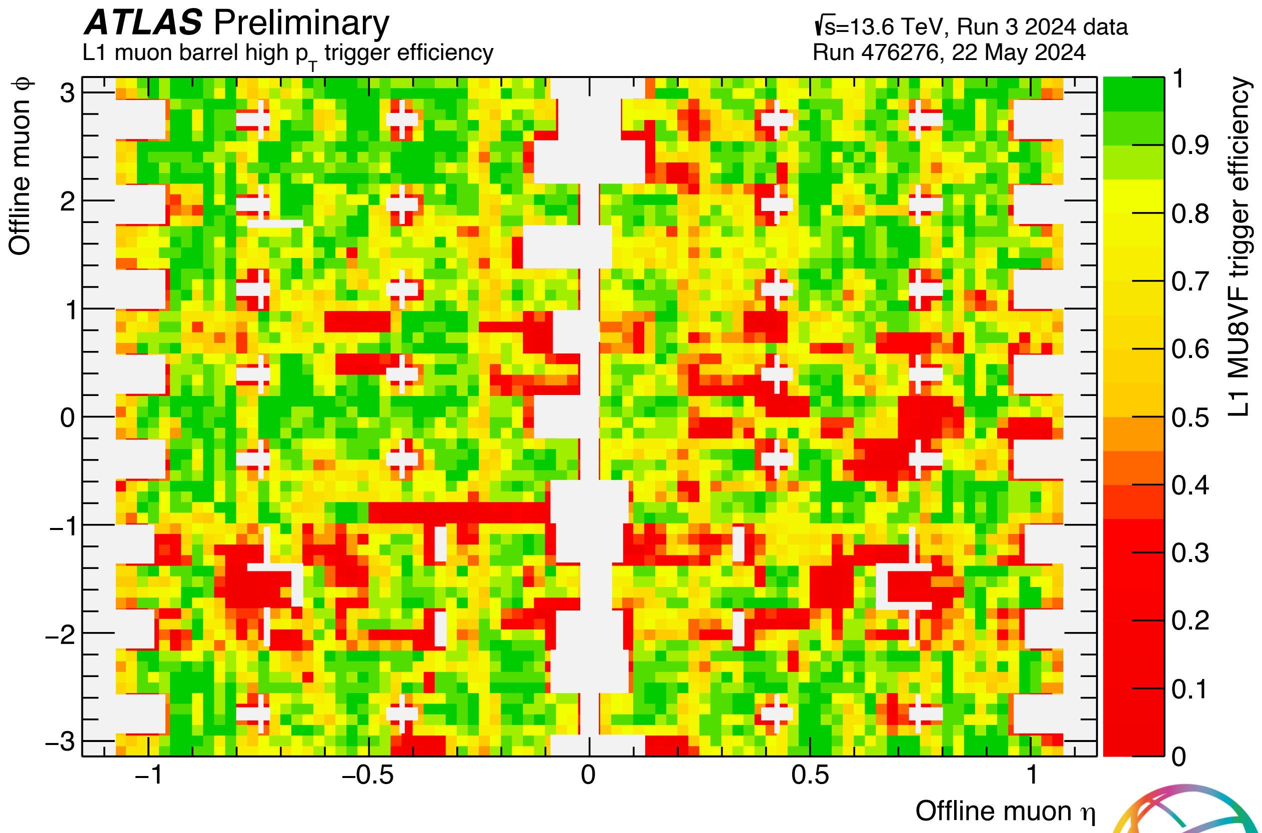

High p_T L1 muon barrel trigger efficiency as a function of the offline muon η and φ for Run 456016 (2023, left) and for Run 476276 (2024, right).

Trigger performance - low p_T $\eta - \varphi$ efficiency maps

- Constant trigger performance between 2023 and 2024 for low p_T triggers.
- Improvement in trigger coverage due to the YETS interventions.

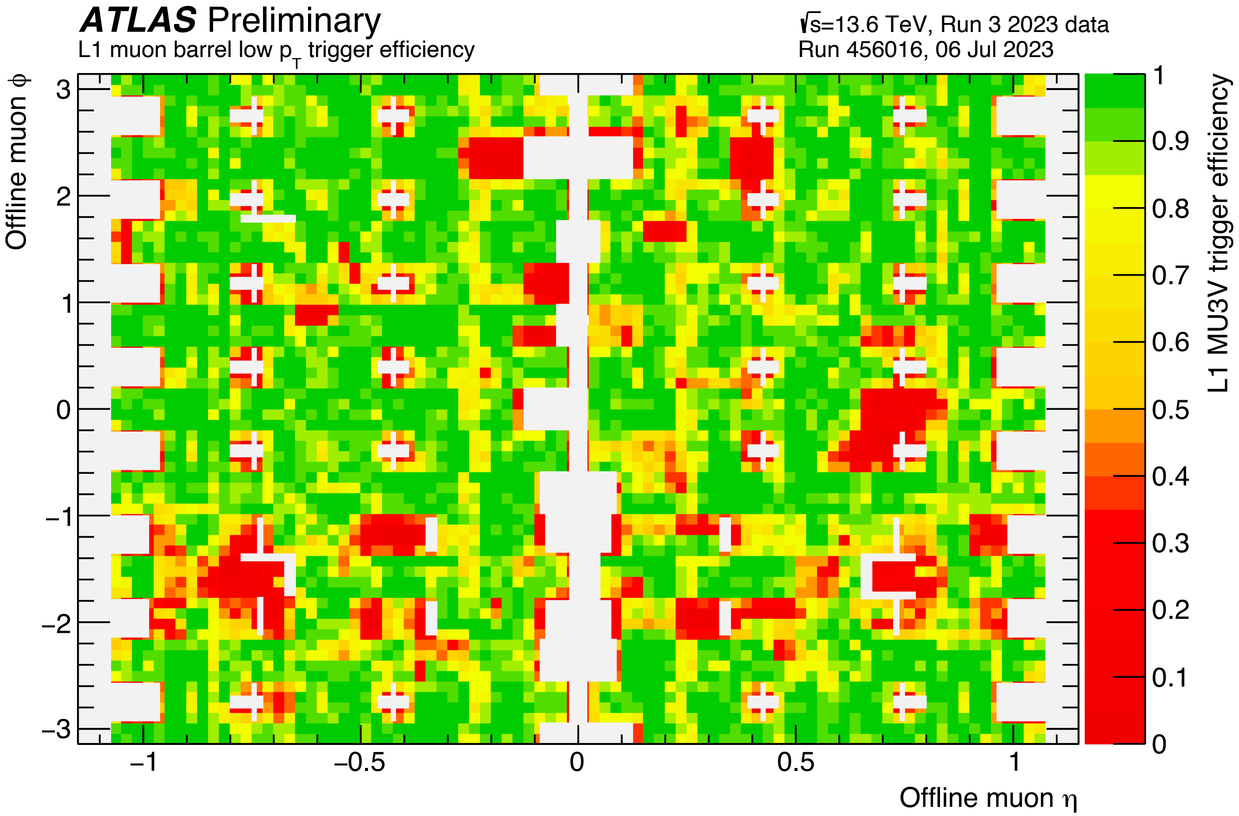

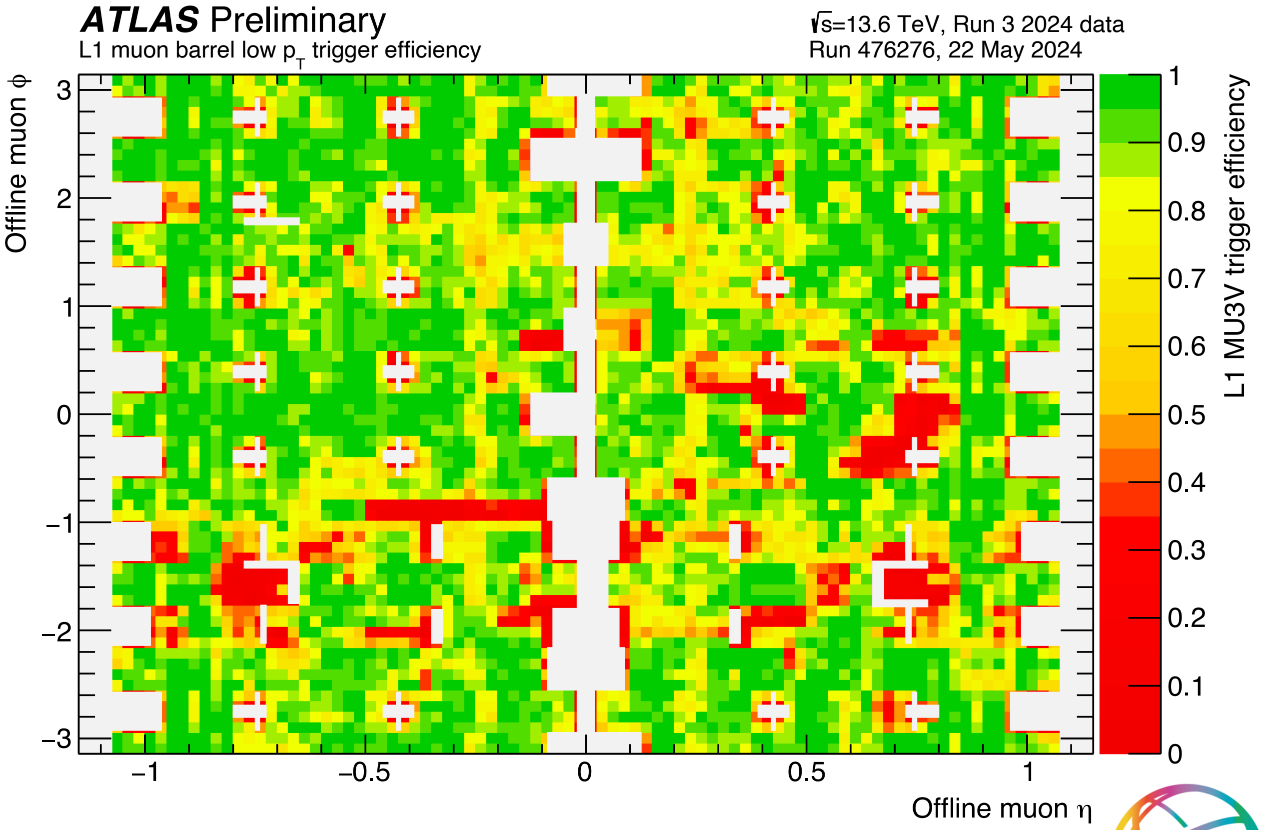

Low p_T L1 muon barrel trigger efficiency as a function of the offline muon η and φ for Run 456016 (2023, left) and for Run 476276 (2024, right).

Conclusions

- RPC detector operating with a new gas mixture since August 2023 at the end of the 2023 *pp* collisions.
- Detector status and performance with the new gas mixture are being monitored/studied.
- The new gas mixture is behaving as expected at detector level, yielding an increase of the gas gap current and a similar cluster size.
- The measured trigger efficiency during 2024 is at a similar level to 2023.
- 2024 operations are progressing well with focus on reducing gas leaks and increasing as much as possible the trigger coverage.

Backup

The ATLAS muon detector during Run3

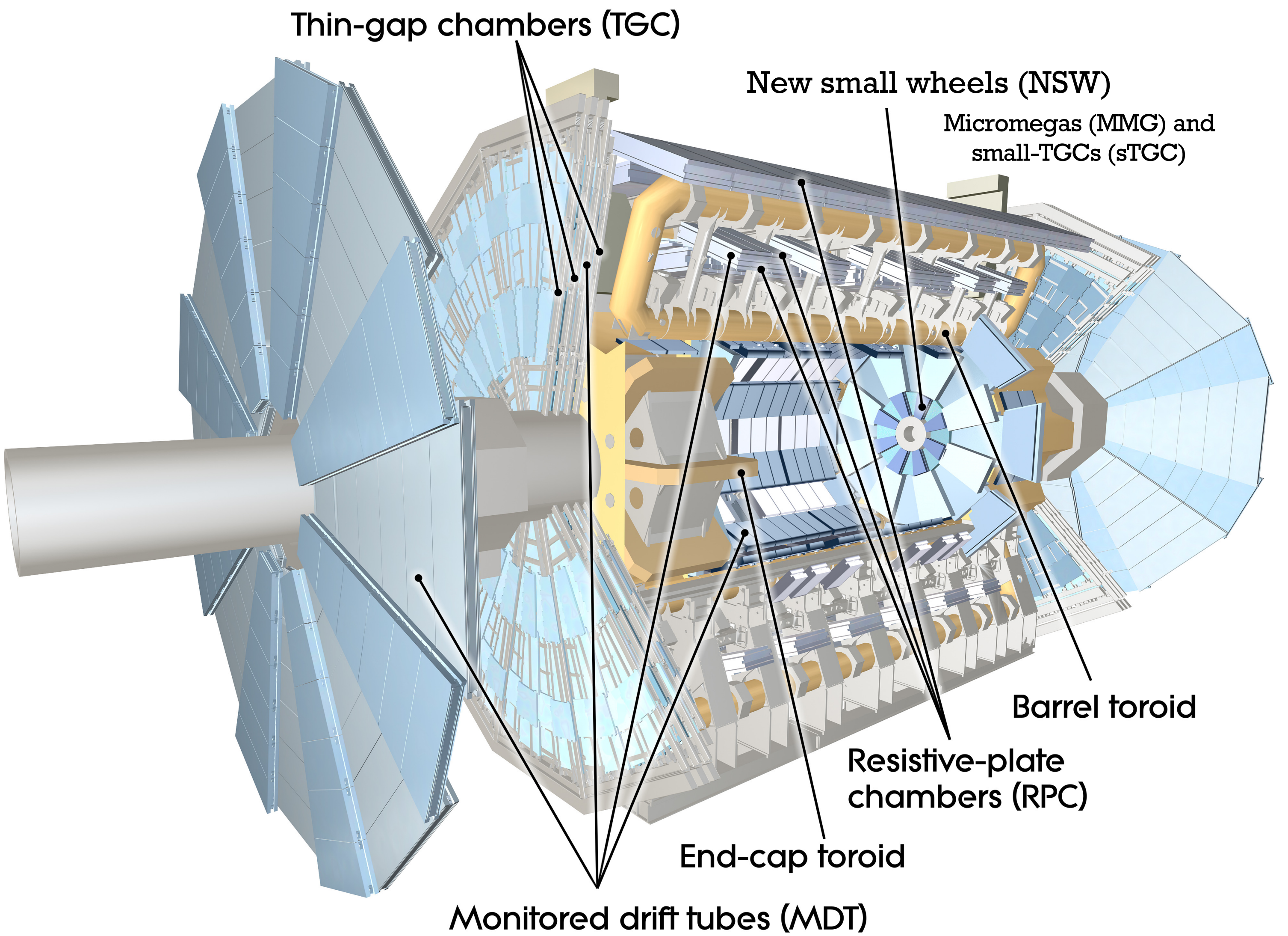

Different muon detectors, each with a specific goal:

- MDT and sMDT to precisely measure the muon momenta.
- RPC and TGC for fast triggering the muons.
- NSW to increase acceptance in the endcaps in high-luminosity conditions.

RPC detector performance during Run2

Measured gas gap current density, mean gas gap current densities and cluster size in 2018 during Run2[1].

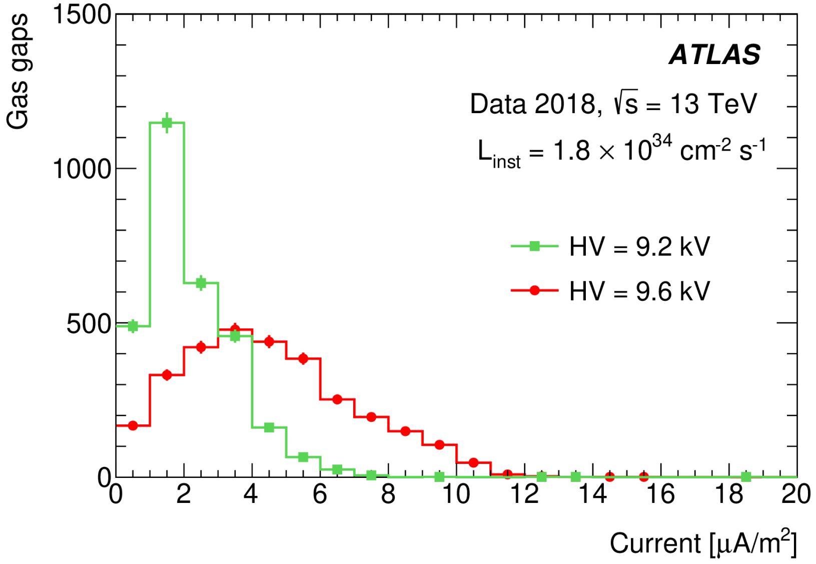

Distributions of the measured current density for the selected RPCs obtained at an instantaneous luminosity of 1.8 × 10 $\mathrm{cm}^{-2}\mathrm{s}^{-1}$. The measurements were taken during one representative run in 2018.

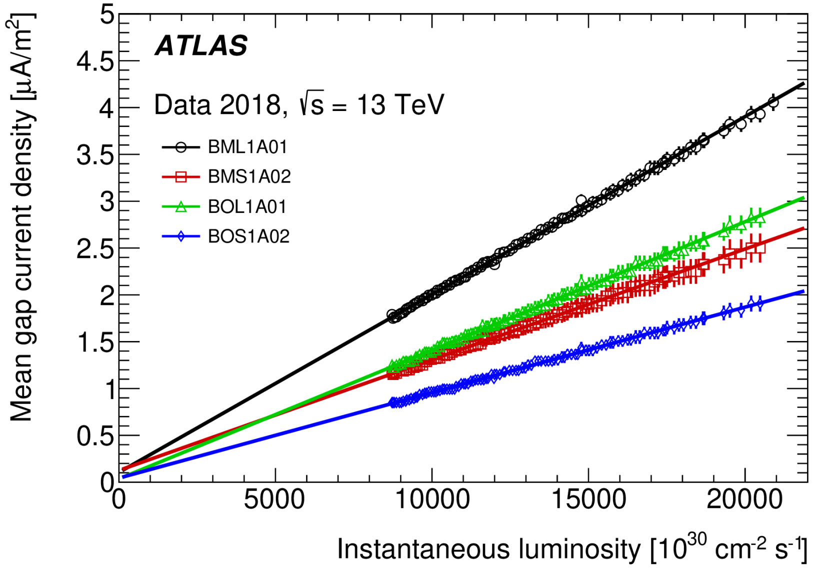

RPC mean gap current density shown as a function of instantaneous luminosity for all the modules in some of the RPC stations.

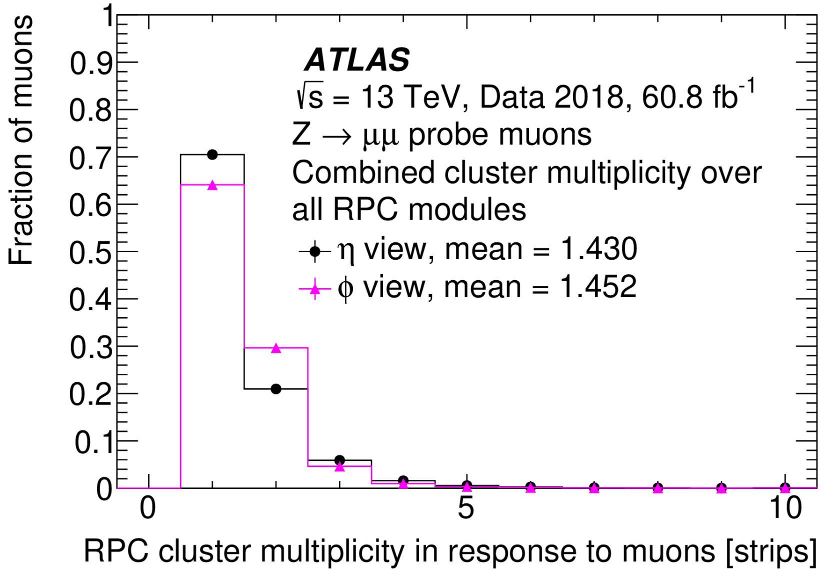

RPC cluster cluster size distribution combined over all RPC modules with η and ϕ panels shown separately.

[1] ATLAS Collaboration, "*Performance of the ATLAS RPC detector and Level-1 muon barrel trigger at $\sqrt{13}$ TeV*", JINST 16 P07029 (2021), https://doi.org/10.1088/1748-0221/16/07/P07029.

RPC trigger performance during Run2

Measured L1 muon barrel efficiency in 2018 during Run2[1].

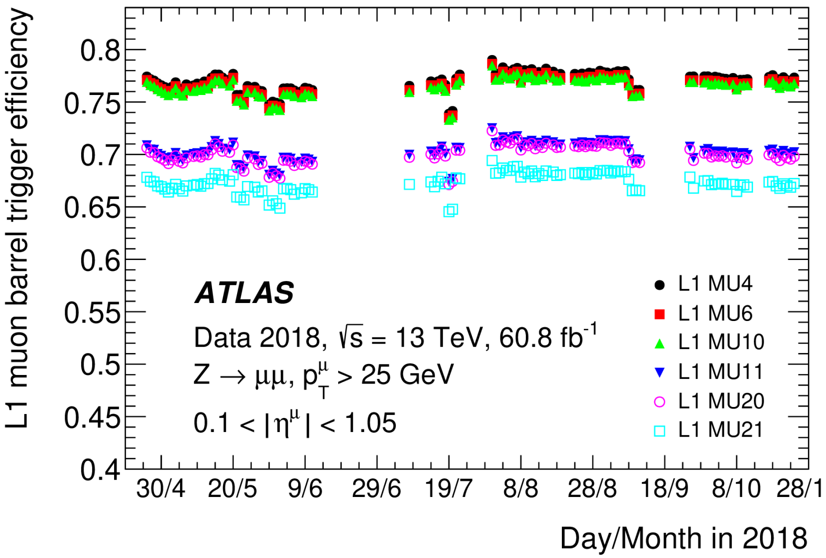

The overall measured L1 muon barrel trigger efficiency as a function of time.

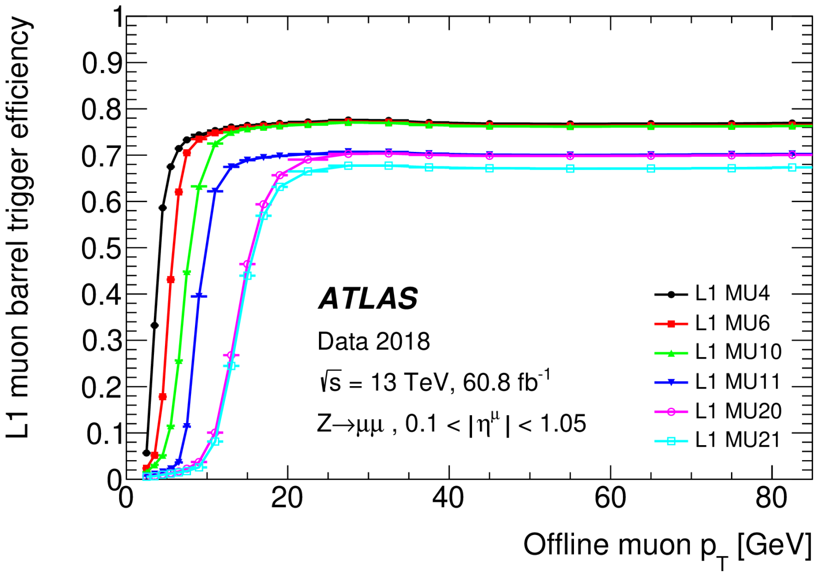

L1 muon barrel trigger efficiency plotted as a function of the probe muon p_{T} .

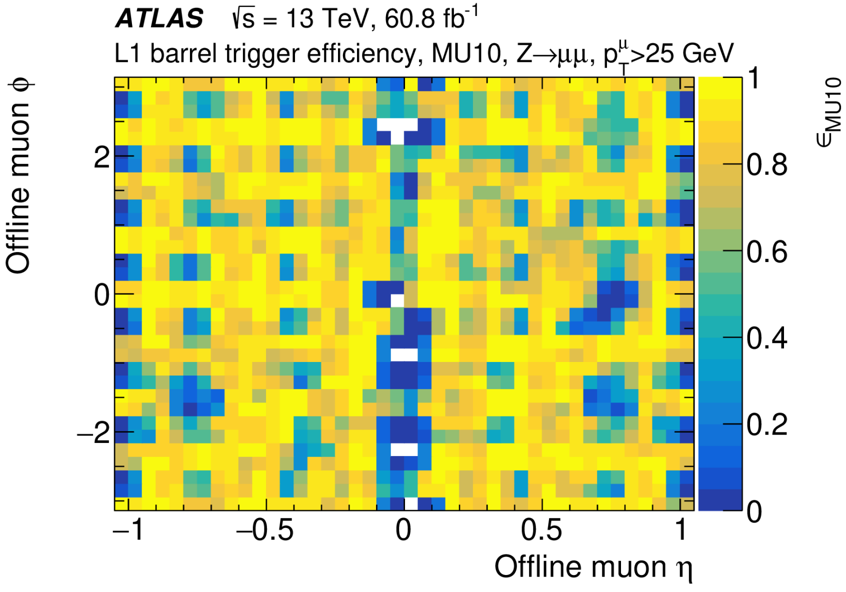

L1 muon barrel trigger efficiency as a function of the muon pseudorapidity and azimuthal angle for the MU10 L1 trigger.

[1] ATLAS Collaboration, "*Performance of the ATLAS RPC detector and Level-1 muon barrel trigger at* $\sqrt{13}$ *TeV*", JINST 16 P07029 (2021), https://doi.org/10.1088/1748-0221/16/07/P07029.

Prototype results

- The performance of RPC detectors operated with different levels of $C_2H_4F_4$, CO_2 and SF_6 was carefully evaluated using prototypes at the CERN Gamma Irradiation Facility in presence of muon beams[2].

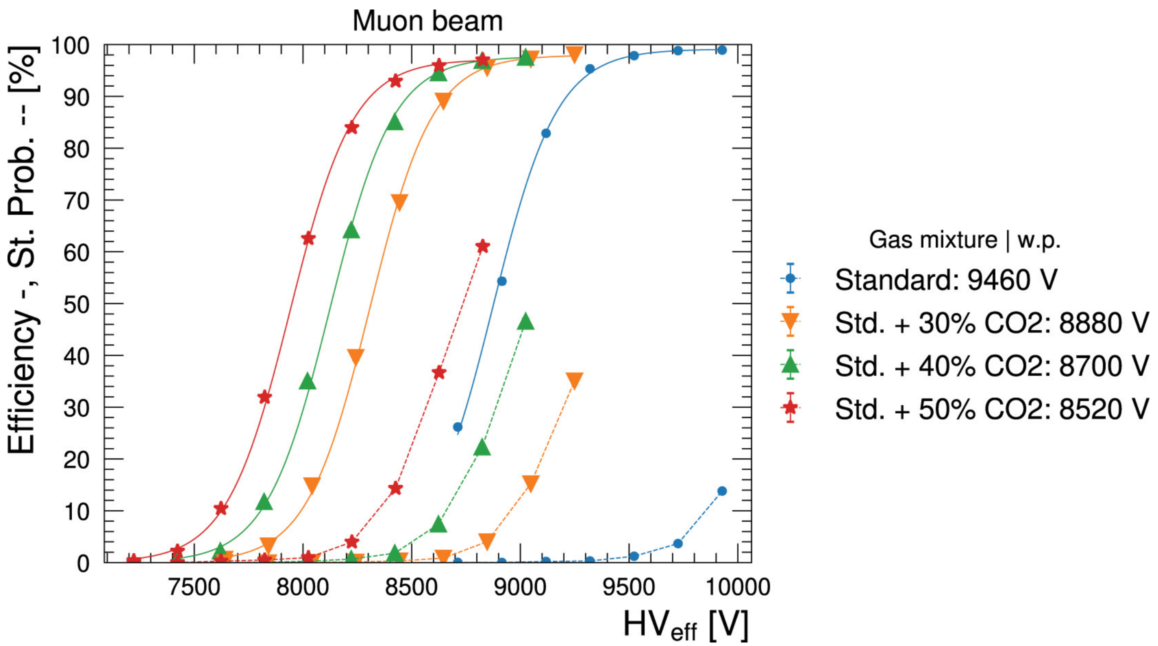

Efficiency (full lines) and streamer probability (dashed lines) curves of the standard gas mixture and the gas mixture with the addition of 30%, 40%, 50% of CO_2.

Gas mixture	Currents	Time resolution
Std.	245 μA ± 1 μA	1.94 ns ± 0.05 ns
30% CO_2 + 0.3% SF_6	292 μA ± 1 μA	1.62 ns ± 0.05 ns
30% CO_2 + 0.9% SF_6	284 μA ± 1 μA	1.60 ns ± 0.05 ns
40% CO_2 + 0.9% SF_6	300 μA ± 1 μA	1.61 ns ± 0.05 ns

Currents and time resolution for different levels of CO_2 and SF_6 gas mixture.

[2] G. Rigoletti, R. Guida, B. Mandelli, "*Performance studies of RPC detectors operated with C2H2F4 and CO2 gas mixtures*", Nucl. Instrum. Methods Phys. Res. Section A, V1049 (2023), https://doi.org/10.1016/j.nima.2023.168088.